ORIGINAL ARTICLE

Abundance of Synaptic Vesicle-Related Proteins in Alpha-Synuclein-Containing Protein Inclusions Suggests a Targeted Formation Mechanism

Amellia McCormack[1] · Damien J. Keating[2] · Nusha Chegeni[1] · Alex Colella[1,3] · Jing Jing Wang[3] · Tim Chataway[1]

Abstract

Proteinaceous α-synuclein-containing inclusions are found in affected brain regions in patients with Parkinson's disease (PD), Dementia with Lewy bodies (DLB) and multiple system atrophy (MSA). These appear in neurons as Lewy bodies in both PD and DLB and as glial cytoplasmic inclusions (GCIs) in oligodendrocytes in MSA. The role they play in the pathology of the diseases is unknown, and relatively little is still known about their composition. By purifying the inclusions from the surrounding tissue and comprehensively analysing their protein composition, vital clues to the formation mechanism and role in the disease process may be found. In this study, Lewy bodies were purified from postmortem brain tissue from DLB cases ($n = 2$) and GCIs were purified from MSA cases ($n = 5$) using a recently improved purification method, and the purified inclusions were analysed by mass spectrometry. Twenty-one percent of the proteins found consistently in the GCIs and LBs were synaptic-vesicle related. Identified proteins included those associated with exosomes (CD9), clathrin-mediated endocytosis (clathrin, AP-2 complex, dynamin), retrograde transport (dynein, dynactin, spectrin) and synaptic vesicle fusion (synaptosomal-associated protein 25, vesicle-associated membrane protein 2, syntaxin-1). This suggests that the misfolded or excess α-synuclein may be targeted to inclusions via vesicle-mediated transport, which also explains the presence of the neuronal protein α-synuclein within GCIs.

Keywords Lewy body · Glial cytoplasmic inclusion · Parkinson's disease · Multiple system atrophy · Vesicle trafficking · Mass spectrometry

Introduction

Parkinson's disease (PD), dementia with Lewy bodies (DLBs) and multiple system atrophy (MSA) are all synucleopathic neurodegenerative diseases. While varying in clinical and pathological presentation, they share a common link—α-synuclein-containing protein inclusions (ASPIs), which are proteinaceous aggregates found in affected brain regions. ASPIs are found in neurons in PD and DLB and are known as Lewy bodies (LBs). In MSA, however, they are found in oligodendrocytes, and thus are termed glial cytoplasmic inclusions (GCIs).

PD is the most common neurodegenerative movement disorder in the world, with incidence increasing with age from 1% of the population at 65 years of age up to 5% at 85 years of age (Alves et al. 2008). PD is neurologically characterised by two main features—the progressive loss of dopaminergic neurons from the substantia nigra (SN) region of the brain (Alves et al. 2008; Tan 2007; Wood-Kaczmar et al. 2006) and the presence of LBs in the surviving neurons (Alves et al. 2008; Fahn 2003; Wood-Kaczmar et al. 2006). The role LBs play in pathology is as yet unknown. DLB is the second most frequent neurodegenerative dementia in the elderly, affecting 0.7% of the population over 65 years (McKeith et al. 2004). Similar to PD, DLB is characterised pathologically by the presence of LBs.

✉ Tim Chataway
tim.chataway@flinders.edu.au

1 Flinders Proteomics Facility, College of Medicine and Public Health, Flinders University, Bedford Park, South Australia 5042, Australia

2 College of Medicine and Public Health, Flinders University, Bedford Park, South Australia 5042, Australia

3 Department of Immunology, Flinders Medical Centre and Flinders University, SA Pathology, Bedford Park, South Australia 5042, Australia

Lewy bodies are eosinophilic aggregates of filamentous structures, resembling neurofilament, and they may also contain vesicular or circular structures. There are two types of LBs—the brainstem (classical) type and the cortical type (Wakabayashi et al. 2007). Brainstem LBs are found in the cytoplasm, with either single or multiple LBs present in a neuron. They are spherical or elongated in shape, with a dense core and a peripheral halo. In contrast, cortical LBs are poorly defined with an irregular shape, often lacking a central core or conspicuous halo (Wakabayashi et al. 2007). LBs are widely distributed throughout the central nervous system (CNS), including in the substantia nigra, hypothalamus, nucleus basalis of Meynert, locus ceruleus, dorsal raphe nucleus, intermediolateral nucleus of the spinal cord and sacral autonomic nucleus (Uversky and Eliezer 2009; Wakabayashi et al. 2007).

While the function of LBs is currently unknown, there are two opposing theories on the relationship between LBs and neuronal loss. The first is that LBs are a toxic aggregation of proteins that contribute directly to neuronal death. The second is that LBs are a protective mechanism that sequesters potentially toxic excess or misfolded α-synuclein that cannot be degraded by the cell (Cordato and Chan 2004). The major constituent of LBs is α-synuclein, including truncated, oxidised and phosphorylated variants (Klein and Schlossmacher 2007) and is estimated to form 8.5% of total protein content (McCormack et al. 2016). There have been more than 70 other proteins identified in LBs, including structural elements of the LB fibrils such as neurofilament and other cytoskeletal proteins such as tubulin; α-synuclein-binding proteins such as 14-3-3 and synphillin-1; components of the ubiquitin–proteasome system; and others (Wakabayashi et al. 2007). However, an ad hoc approach has been taken to the identification of these components.

While MSA is less prevalent than PD (Wenning et al. 2008), it typically affects patients at a younger age with a shorter survival (Wenning et al. 1997; Yoshida 2007). MSA features neuronal cell loss and gliosis (Vanacore et al. 2001; Vanacore 2005) and is pathologically characterised by the presence of GCIs in the cytoplasm of oligodendrocytes (Vanacore 2005; Wakabayashi and Takahashi 2006; Wenning et al. 2008). GCIs are filamentous structures, consisting of a loosely packed meshwork of granular-coated fibrils (Wenning et al. 2008). GCIs can be either sickle, triangular, half moon, oval or conical in shape and are both argyrophilic and eosinophilic (Yoshida 2007). In oligodendrocytes that contain GCIs, the nuclei are slightly larger than in non-GCI-bearing cells (Inoue et al. 1997).

GCIs are widely distributed throughout the CNS. They appear more frequently in white matter than in grey matter. Areas of the CNS that contain a higher density of GCIs are the subcortical areas of the motor cortex, pre-motor cortex and supplementary motor areas, and the dorsolateral putamen (Inoue et al. 1997). Even in the earliest stages of MSA,

GCIs are present. They increase in abundance as the disease progresses, with a correlation between GCI frequency and the severity of olivopontocerebellar degeneration. This is unlike PD and DLB, where the frequency of LBs does not correlate with the degree of striatonigral degeneration. At the advanced stage of MSA, with severe cerebellar devastation, GCIs are absent altogether (Inoue et al. 1997).

α-Synuclein is thought to be the most abundant protein present in GCIs (Ozawa 2006; Wakabayashi and Takahashi 2006; Wenning et al. 2008) consisting of 11.7% of total protein content (McCormack et al. 2016). The form present in GCIs is misfolded and relatively insoluble, with predominant oxidative and nitrative modifications (Ozawa 2006). This accumulation of α-synuclein in oligodendrocyte inclusions is unexpected, as α-synuclein is a neuronal protein that is expressed transiently in developing oligodendrocytes but not in the mature cells (Culvenor et al. 2002; Richter-Landsberg et al. 2000). The presence of full-length α-synuclein in the CSF provides evidence that it is released extracellularly from neurons (Borghi et al. 2000), but it is still unknown how or why it accumulates in GCIs in oligodendrocytes. Other proteins found in GCIs include tubulin polymerisation promoting protein (TPPP), also known as p25 (Lindersson et al. 2005), rab3, a member of the Ras family of small GTP-binding proteins, 14-3-3 protein, heat shock protein 90, and DJ-1, which is implicated in PD (Ozawa 2006).

A detailed account of the composition of ASPIs could assist in understanding the biology of their formation and their role in the disease process. However, the comprehensive proteomic analysis of ASPIs has been limited by the ability to isolate these inclusions with sufficient purity and yield from the surrounding structures in postmortem tissue. We have recently described a method to isolate LBs and GCIs with high purity and yield (McCormack et al. 2016), and here, we examine the protein composition of highly enriched LBs and GCIs through mass spectrometry (MS) and immunohistochemistry and identify an enrichment of vesicle and vesicle-related proteins within these ASPIs.

Materials and Methods

Brain Tissue Specimens

Fresh-frozen brain tissue was obtained from the South Australian Brain Bank, Adelaide, with ethics approval received from the Flinders Clinical Research Ethics Committee (Approval 06/067). The brain tissue had been extracted within a 36-h postmortem interval and bisected at the midsagittal plane in a dry ice bath, with one half snap-frozen for later use and the other half aldehyde-fixed, blocked and embedded in paraffin for subsequent neuropathological assessment by SA Pathology, Adelaide, Australia. Pathology

reports for each case guided targeting of tissues for ASPI purification. Specimens of MSA and DLB cases were utilised in this study (see Table 1).

Brain Tissue Homogenisation

Tissue sections containing ASPIs were thawed on ice, dissected at 4 °C and divided into 2 g lots. Each lot was mixed with 8 mL of homogenisation buffer (20 mM tris, 0.32 M sucrose, 0.05% (w/v) sodium azide, 5 mM EDTA, 1 µg/mL pepstatin, 1 µg/mL leupeptin, 0.3 mM PMSF, pH 7.4) and homogenised in a Dounce homogeniser for 20 strokes with Pestle A (loose) then 20 strokes with Pestle B (tight). Homogenised tissue from the same case was pooled and mixed, then divided into 10-mL tubes and snap-frozen in liquid nitrogen. Brain homogenate was stored at − 80 °C.

ASPI Purification

ASPIs were purified from homogenised brain tissue according to the method of McCormack et al. (2016). GCIs were purified from MSA basal ganglia, from the equivalent of 4 g of MSA 1, 5 g of MSA 2, 3 g of MSA 3, 5 g of MSA 4 and 4 g of MSA 5 tissue. Purified GCIs were used from each of these samples for subsequent mass spectrometry analysis. Further GCIs were purified from the equivalent of 6 g of MSA 1 basal ganglia for 1D gel analysis, and from 6 g of pooled MSA 1 and MSA 6 basal ganglia for 2D gel analysis.

LBs were purified from DLB brainstem from the equivalent of 6 g of DLB 1 and 6 g of DLB 2 tissue. The purified LBs were used from each of these samples for subsequent mass spectrometry analysis.

Sample Preparation and Quantitation

EZQ Protein Quantitation Assays were performed according to the manufacturer's instructions (Invitrogen). For samples

intended for 1-DE and 2-DE, ReadyPrep 2-D Protein Clean-Up of samples were performed on solubilised purified GCIs according to the manufacturer's instructions (BioRad). For 1-DE, the sample was subsequently solubilised in 1× 1D sample buffer without bromophenol blue (62.5 mM Tris-HCl, 10% (v/v) glycerol, 2% (w/v) SDS, 100 mM DTT, pH 6.8), vortexed and heated at 95 °C for 5 min. The sample was vortexed again, spun at 18,000×g and the supernatants collected for 1-DE. For 2-DE, the sample was subsequently solubilised in protein extraction buffer (7 M urea, 2 M thiourea, 4% (w/v) CHAPS).

For samples intended for direct MS analysis, 20 µg of solubilised purified GCIs from each of the five MSA cases and 20 µg of solubilised purified LBs from each of the two DLB cases were directly buffer-exchanged into 50 mM ammonium bicarbonate using Vivaspin 500 5 kDa MWCO columns (GE Healthcare), according to the manufacturer's instructions.

1D Gel Electrophoresis

1D SDS PAGE was performed using precast Mini-Protean® TGX™ Any kD™ gels (BioRad). An 18 µg sample of purified GCIs was diluted into 1× 1D sample buffer containing freshly added DTT (62.5 mM Tris-HCl, 10% (v/v) glycerol, 2% (w/v) SDS, 100 mM DTT, 0.01% (w/v) bromophenol blue, pH 6.8) and heated at 90 °C for 5 min, then loaded onto the gel. Gels were electrophoresed at 200 V at constant voltage in a Biorad Mini-Protean Tetra electrophoresis system until the bromophenol blue dye front reached 0.5 cm from the bottom edge of the gel.

2D Gel Electrophoresis

2D gel electrophoresis was performed using cup loading isoelectric focusing according to the 2D Electrophoresis Principals and Methods Handbook 80-6429-60AC (GE Healthcare). A 24 cm Immobiline DryStrip gel pH 3–11 NL (GE Healthcare) was passively rehydrated overnight in 475 µL of isoelectric focusing (IEF) rehydration buffer (7 M urea, 2 M thiourea, 4% (w/v) CHAPS, 0.5% (v/v) IPG Buffer, 0.4% (w/v) DTT) using an Ettan IPGphor 3 IEF unit (GE Healthcare). The strip was then placed gel side up in an IPGphor Manifold (GE Healthcare) and the manifold set up for cathodic cup loading accordingly to the manufacturer's instructions. Two hundred fifty micrograms of solubilised inclusions, purified using a 2D Clean-up Kit (BioRad), were applied to the strip. Isoelectric focusing was performed overnight according to the following protocol: step to 200 V for 1 h, step to 400 V for 1 h, step to 800 V for 2 h, linear gradient to 8000 V for 1 h, hold at 8000 V until 40,000 Vhr, step to 400 V and hold until removed from the apparatus, which was 52,000 Vhr.

Table 1 Case details for postmortem brain tissue used

Case	Area	Gender	Age[a]	PMI[b]
DLB 1	Brainstem	F	81	12
DLB 2	Brainstem	M	73	34
DLB 3	Superior frontal	M	80	6
MSA 1	Basal ganglia, superior temporal	M	73	20
MSA 2	Basal ganglia	F	62	8
MSA 3	Basal ganglia	F	81	17
MSA 4	Basal ganglia	F	73	5
MSA 5	Basal ganglia	M	59	13
MSA 6	Basal ganglia, cerebellum	F	77	5

[a] Age at time of death (years)

[b] Postmortem interval (h)

Second dimension SDS-PAGE was carried out according to the 2D Electrophoresis Principals and Methods Handbook 80-6429-60AC (GE Healthcare). The strips were equilibrated in 10 mL of equilibration solution 1 (100 mM tris-HCl, 6 M urea, 30% (v/v) glycerol, 2% (w/v) SDS, 1% (w/v) DTT, pH 8.0) for 15 min at room temperature with gentle agitation, followed by 15 min in 10 mL of equilibration solution 2 (100 mM tris-HCl, 6 M urea, 30% (v/v) glycerol, 2% (w/v) SDS, 4% (w/v) iodoacetamide, 0.003% (v/v) bromophenol blue solution, pH 8.0).

Each equilibrated strip was applied to the top of a 24 cm 12.5% linear gel (labcast using a GE Healthcare Ettan DALTsix gel caster) and sealed with 1% low melting point agarose solution (25 mM Tris, 192 mM glycine, 0.06% (w/v) SDS, 1% (w/v) low melting point agarose, pH 8.3), which was set at 4 °C for 5 min. The gels were run on an Ettan DALTsix electrophoresis unit (GE Healthcare) with a MultiTemp III external thermostatic circulator (GE Healthcare) set to 10 °C. The gels were run at constant power at 2 W per gel for 45 min, then at 17 W per gel until the bromophenol blue dye front reached 0.5 cm from the bottom edge of the gels.

Gel Imaging and Staining

SyproRuby staining was performed according to the manufacturer's instructions (BioRad). Imaging was performed on a Typhoon 9400 variable mode imager at 200 μm resolution using a blue 457 nm laser, 610 BP emission filter and PMT value of 600 V (1D gel) or 700 V (2D gel). Subsequent silver staining was performed to visualise bands/spots to excise for tryptic digestion. Silver staining was performed using an MS-compatible Erichrome black T (EBT)-silver method, as described by Jin et al. (2006).

In-Gel Tryptic Digestion of 1D Gel Slices

Tryptic digestion of 1D gel slices was performed based on the method of Link and LaBaer (2009). The gel was washed in dH$_2$O three times for 30 min per wash, to remove traces of acetic acid from the fixative. Bands of interest were excised using a scalpel, diced into 1 mm^2 pieces, and placed into the wells of a 96-well plate.

The gel pieces were washed in 150 μL 50% acetonitrile (ACN):dH$_2$O for 15 min. The wash was removed, and 150 μL of 100% ACN was added to shrink the gel pieces. The pieces were rehydrated in 75 μL 100 mM ammonium bicarbonate for 5 min, then 75 μL of ACN was added and the pieces were incubated for 15 min. The wash was removed, and 150 μL of 100% ACN was added to shrink the gel pieces.

The gel pieces were rehydrated in 150 μL of 10 mM DTT in 100 mM ammonium bicarbonate solution and incubated for 45 min at 65 °C. The DTT solution was removed, and 150 μL of 50 mM iodoacetamide in 100 mM ammonium bicarbonate was added immediately and incubated for 30 min at 30 °C in the dark. The iodoacetamide solution was removed, and the gel pieces were washed in 150 μL of 50% ACN:dH$_2$O for 15 min. The wash was removed, and 150 μL of 100% ACN was added to shrink the gel pieces.

Trypsin stock solution (1 μg/μL Trypsin Gold mass spectrometry grade, Promega) was diluted 100-fold (0.01 μg/μL) in 50 mM ammonium bicarbonate. The gel pieces were rehydrated in 28 μL (0.28 μg) of trypsin solution for 30 min at room temperature, then incubated at 37 °C for a minimum of 4 h.

In-Gel Tryptic Digestion of 2D Gel Spots

Tryptic digestion of 2D gel spots was performed based on the method of Link and LaBaer (2009). Gel spots were excised from a 2D gel using a truncated low protein-binding 200 μL pipette tip attached to OneTouch Plus Spot Picker. The cutting tip was rinsed in 100% ethanol between each spot to minimise cross-contamination. Each spot was placed in a separate well of a 96-well plate, and any residual liquid was removed. Using a Biomek® 3000 laboratory automation workstation (Beckman Coulter), 150 μL of 100 mM ammonium bicarbonate was pipetted into each well, and the plugs were washed with shaking at an amplitude of 6 on a DPC Micromix 5 mixing platform for 30 min. The ammonium bicarbonate was removed and 150 μL of acetonitrile was pipetted into each well and left overnight to dehydrate the gel plugs.

The plugs were rehydrated with 150 μL of 100 mM ammonium bicarbonate and washed with shaking for 30 min. One hundred thirty microliters of the wash was removed and replaced with 130 μL of fresh 100 mM ammonium bicarbonate and washed for a further 30 min. All liquid was removed, and the plugs were washed with 150 μL of 50% ACN:dH$_2$O for 30 min. One hundred thirty microliters of the wash was removed and replaced with 130 μL of fresh 50% ACN:dH$_2$O and washed for a further 30 min. All liquid was removed, and 150 μL of ACN was pipetted into each well and left overnight to dehydrate the gel plugs.

Trypsin stock solution (1 μg/μL Trypsin Gold mass spectrometry grade, Promega) was diluted 100-fold (0.01 μg/μL) in 50 mM ammonium bicarbonate. Each gel plug was rehydrated in 28 μL (0.28 μg) of trypsin solution for 30 min at room temperature, then incubated at 37 °C for a minimum of 4 h.

In-Solution Tryptic Digestion of Complex Samples

In-solution tryptic digestion was based on the method on the method of Link and LaBaer (2009). A 1/10 volume of 50 mM DTT was added and incubated for 5 min at 65 °C to reduce disulphide bonds. A 1/10 volume of 100 mM iodoacetamide was added and incubated for 30 min at 30 °C in the dark to alkylate sulphhydral residues and prevent the reformation of the

disulphide bonds. Trypsin (Trypsin Gold mass spectrometry grade, Promega) was added at a 1:50 trypsin to protein ratio, and the sample was incubated at 37 °C for a minimum of 4 h.

HPLC Linear Ion Trap/FTMS Mass Spectrometry

The digested peptides obtained from either complex mixtures or gel pieces were analysed with a Thermo LTQ Orbitrap XL mass spectrometer (Thermo Fisher Scientific, Waltham, MA, USA) fitted with a nanospray source. One to 5 μL of each sample was drawn into a 20-μL loop with buffer on either side using a custom inject program and loaded onto an Acclaim® PepMap 100 C18 cartridge (Dionex, Sunnyvale, CA, USA) at 5 μL/min for 12 min, then separated on a packed nanocapillary column NTCC-360/100-5-153 (Nikkyo Technos, Tokyo, Japan) at 200 nL/min using an Ultimate 3000 HPLC (Dionex) with a gradient from 0 to 40% Buffer B over 52 min, followed by 95% Buffer B for 16 min, followed by 100% Buffer A for 30 min. The mass spectrometer was operated in positive ion mode with one full scan of mass/charge (m/z) 300–2000 in the FTMS analyser, with ions possessing a charge state of 1 rejected, followed by product ion scans of the six most intense ions in the ion trap analyser, with dynamic exclusion of 15 s with a repeat duration of 15 s, an exclusion list of 500 proteins, and collision-induced dissociation energy of 35%.

Protein Identification

The MS spectra were searched with Thermo Proteome Discoverer (PD) version 1.2.0.208 based on the method by Wilson et al. (2011) using the Sequest algorithm against the Uniprot human (taxonomy 9606) with isoforms database version August 2011. The search parameters were as follows: trypsin as the protease with up to two missed cleavages; mass tolerance for peptide identification of precursor and product ions of 15 ppm and 0.8 Da, respectively; and variable modifications of carbamidomethylation and nitrosylation of carbons, oxidation of methionines, ubiquitination of lysines, and phosphorylation of serines, threonines and tyrosines. The filters were peptides of a high confidence value, count only rank 1 peptides, count peptide only in top scored proteins and at least two unique peptides sequenced for each protein. The false discovery rate (FDR) was calculated for each complex mixture analysis using the FDR algorithm in PD. The FDR was less than 1% for all samples analysed.

Immunofluorescence

Immunofluorescence was performed on fixed sections of MSA 1 tissue (superior temporal region) and DLB 3 tissue (superior frontal region). The slides were deparraffinised with the following protocol: xylene for 10 min × 2, 100% ethanol for 5 min × 2, 95% ethanol for 5 min, 70% ethanol for 5 min, dH₂O for 5 min. Antigen retrieval was then performed by immersing the slides in an antigen retrieval tank filled with 1 mM EDTA pH 8.0 and microwaved on medium power for 10 min, followed by washing in TBS-Azide (20 mM tris, 150 mM NaCl, 0.1% (w/v) sodium azide, pH 7.4) for 2 min.

The following steps were carried out in a humidifying chamber at room temperature. The slides were incubated in hydrogen peroxide solution (1% H_2O_2 + 50% methanol in dH₂O) for 30 min to eliminate endogenous peroxidase activity. The slides were then washed with a transfer pipette three times for 5 min each with TBS-Azide. The slides were blocked for 60 min with blocking solution (20 mM Tris, 150 mM NaCl, 0.1% (w/v) sodium azide, 20% (v/v) normal horse serum, pH 7.4) and then incubated for 2 h in primary antibody diluted in antibody diluent (20 mM tris, 150 mM NaCl, 0.1% (w/v) sodium azide, 1% (v/v) normal horse serum, pH 7.4). Dual staining was performed using a sheep polyclonal anti-α-synuclein primary antibody (Gai et al. Adelaide, Australia) used at 1:1000 (1 μg/mL) with either (a) a rabbit polyclonal anti-SNAP25 primary antibody (Osenses, Cat. No. OS-219) used at 1:500, (b) a rabbit polyclonal anti-VAMP2 primary antibody (Osenses, Cat. No. OS-222) used at 1:500, (c) a rabbit polyclonal anti-synaptotagmin-1 primary antibody (Osenses, Cat. No. OS-213) used at 1:250 or (d) a rabbit polyclonal anti-synaptophysin primary antibody (Osenses, Cat. No. OS-209) used at 1:250.

Slides were then washed three times for 5 min each with TBS-Azide, then incubated in fluorescent-conjugated secondary antibodies diluted in antibody diluent for 60 min. Cy-3-conjugated AffiniPure Donkey Anti-Sheep secondary (Jackson Laboratories, Cat. No. 713-165-147) and Alexa Fluor 488 conjugated Donkey Anti-rabbit secondary (Invitrogen, Cat. No. A-21206) were both used at 1:200 (3.75 μg/mL and 5 μg/mL, respectively). The slides were washed three times for 5 min each with TBS-Azide and coverslipped with Vectashield Mounting Medium with DAPI for nuclei staining.

Samples were viewed and photographed on an Olympus BX50 Fluorescence microscope, and channels were colourised and merged in Adobe Photoshop (version CS5), using blue (hue 225) for DAPI, green (hue 105) for Cy3 and red (hue 345) for Alexa488.

Results

MS Identification from Complex Mixtures

LB and GCI purifications were performed on tissue from two DLB cases and five MSA cases, respectively, using a recently optimised ASPI purification method (McCormack et al. 2016). Twenty micrograms of each sample was solubilised

and digested with trypsin. The digested peptides were analysed by nanospray mass spectrometry, with two replicates for each of the two samples.

From the four injections of solubilised LBs, a total of 348 proteins were identified. One hundred seventy-four of these proteins (50%) were present in both cases (see Online Resource 1). Thirty protein isoforms (protein variations arising from the same gene family) of 12 proteins previously established to be in LBs (as summarised in Licker et al. 2009 and Leverenz et al. 2007) were identified in both cases: α-synuclein, α-β-crystallin, 14-3-3 proteins, tubulin, neurofilament, alpha-internexin, HSP90, MAP1B, MAP2, agrin, UCH-L1, and CAMK2. A further 9 protein isoforms of 7 proteins previously established to be in LBs were identified in a single case: HSP70, MAP1A, gelsolin, tropomyosin, synaptotagmin, GAPDH and superoxide dismutase.

From the ten injections of solubilised GCIs, a total of 502 proteins were identified. One hundred sixty-four of these proteins were present in a minimum of 4 out of the 5 cases (see Online Resource 2). Twenty protein isoforms of 6 proteins previously established to be in GCIs (as summarised in Wenning et al. 2008) were identified in all five cases: α-synuclein, α-β-crystallin, 14-3-3 proteins, tubulin, MAP1B, and HSP7012A. A further 4 proteins previously established to be in GCIs were identified in one to three cases: MAP2, TPPP (3 cases); MAP1A (2 cases); and CA2 (1 case).

From the solubilised LBs, 55 synaptic vesicle-related proteins were identified, including 9 established synaptic vesicle proteins, 37 proteins transiently associated with the synaptic vesicle membrane and 9 putative novel synaptic vesicle proteins (Table 2). From the solubilised GCIs, 90 synaptic vesicle-related proteins were identified, including 15 established synaptic vesicle proteins, 56 proteins transiently associated with the synaptic vesicle membrane and 19 putative novel synaptic vesicle proteins (Table 3). Of the proteins identified in 2 out of 2 LB cases, 21% were synaptic vesicle-related, and of the proteins identified in ≥ 4 out of 5 MSA cases, 21% were also synaptic vesicle-related. The classification of these identifications is based on a review of the synaptic vesicle proteome by Burre and Volknandt (2007), where proteins were classified as being 'established synaptic vesicle proteins', 'proteins transiently association with the synaptic vesicle membrane during the vesicle life cycle' and 'putative novel synaptic vesicle proteins'. This classification scheme is used throughout this paper.

1D Fractionation of GCI Proteins

1D fractionation of purified GCIs was performed to provide additional coverage to the proteins identified by MS, as the altered solubilisation conditions could provide additional protein identifications. The 1D lane was cut into ten fractions, which were each digested with trypsin and the digested

peptides were analysed by MS. From the ten fractions, 117 proteins were identified (excluding cytokeratins), of which 25 proteins were not identified from the in-solution digestions (see Online Resource 3). Three proteins previously established to be in GCIs were identified: α-synuclein, 14-3-3 proteins (6 isoforms) and tubulin (8 isoforms forms). α-β-Crystallin was not identified. There were 13 synaptic vesicle-related proteins identified, including the 3 established synaptic vesicle proteins synaptotagmin 1, vesicle-associated membrane protein 2, and v-type proton ATPase subunit a, and 10 proteins transiently associated with the synaptic vesicle membrane.

2D Profile of GCI Proteins

Purified GCIs were also subjected to 2-DE to provide additional protein coverage. All visible spots were digested with trypsin and the digested peptides analysed by nanospray mass spectrometry (Fig. 1, spots where a high confidence protein identification was made are shown, spots which contain insufficient protein coverage are omitted). One hundred thirty-five variants of 99 different proteins were identified (see Online Resource 4) from a total of 209 spots. 5 proteins previously established to be in GCIs were identified: α-synuclein, α-β-crystallin, 14-3-3 proteins, tubulin and transferrin. There were ten synaptic vesicle-related protein identifications, including five proteins transiently associated with the synaptic vesicle membrane and five putative novel synaptic vesicle proteins (data not shown). While no established synaptic vesicle proteins were identified from the analysed spots, several proteins with a protein trafficking function were identified, including: alpha- and beta-soluble NSF attachment proteins; sorting nexin-30; transmembrane emp24 domain-containing proteins 2 and 10; and vesicle-fusing ATPase.

Validation of Key Vesicle Protein Identifications

Immunofluoresence was performed on fixed sections of tissue from DLB and MSA cases to confirm the mass spectrometry identifications of the established synaptic vesicle-related proteins synaptosomal-associated protein 25 (SNAP25), vesicle-associated membrane protein 2 (VAMP2), synaptotagmin-1 and synaptophysin in both LBs and GCIs. These proteins were selected for validation based on their classification as established synaptic vesicle-related proteins and commercial antibody availability. The presence of all four proteins was confirmed in both LBs and GCIs (see Fig. 2). However, synaptophysin was not detected via mass spectrometry in the two DLB samples.

Table 2 MS/MS results of proteins from immunocaptured Lewy bodies (LBs) that are synaptic vesicle-related proteins

Protein identified	Accession no.	No. of cases**	Coverage (%)	No. of peptides	Score	pI	MW (kDa)
A: Established synaptic vesicle proteins							
Synaptosomal-associated protein 25*	P60880	2	24.6	3.8	19.4	4.77	23.3
Vesicle-associated membrane protein 2*	P63027	2	28.5	2.0	9.8	8.13	12.7
Synaptic vesicle glycoprotein 2A	Q7L0J3	2	3.1	2.0	8.8	5.57	82.6
V-type proton ATPase catalytic subunit A	P38606	2	15.6	5.5	42.6	5.52	68.3
V-type proton ATPase subunit d 1	P61421	2	21.6	3.8	30.5	5.00	40.3
V-type proton ATPase subunit B, brain isoform	P21281	2	10.2	3.3	21.1	5.81	56.5
Synaptotagmin-1*	P21579	1	6.6	2.0	6.4	8.12	47.5
V-type proton ATPase subunit E 1	P36543	1	15.9	3.0	11.8	8.00	26.1
V-type proton ATPase subunit H	Q9UI12	1	6.6	2.0	7.9	6.48	55.8
B: Transiently associated with the synaptic vesicle membrane							
Actin, cytoplasmic 1	P60709	2	35.6	7.0	133.7	5.48	41.7
Alpha-internexin	Q16352	2	17.1	6.5	76.2	5.40	55.4
AP-2 complex subunit beta	P63010	2	5.7	2.7	16.3	5.38	104.5
Beta-soluble NSF attachment protein	Q9H115	2	35.4	7.0	38.4	5.47	33.5
Calcium/calmodulin-dependent protein kinase II alpha	Q8IWE0	2	10.5	2.7	17.3	7.20	54.1
Calcium/calmodulin-dependent protein kinase type II subunit delta	Q13557	2	11.5	3.3	22.7	7.25	56.3
Clathrin heavy chain 1	Q00610	2	0.1	10.3	75.3	5.69	191.5
Cytoplasmic dynein 1 heavy chain 1	Q14204	2	2.9	8.5	95.8	6.40	532.1
Dynamin-1	Q05193	2	9.7	5.7	31.9	7.17	97.3
Heat shock protein HSP 90-alpha	P07900	2	20.6	12.0	97.9	5.02	84.6
Heat shock protein HSP 90-beta	P08238	2	24.1	13.8	121.9	5.03	83.2
Microtubule-associated protein 1B	P46821	2	8.7	13.5	86.2	4.81	270.5
Neurofilament heavy polypeptide	P12036	2	7.9	6.0	71.2	6.18	112.4
Neurofilament light polypeptide	P07196	2	22.9	9.0	108.6	4.65	61.5
Neurofilament medium polypeptide	P07197	2	25.7	14.3	134.8	4.91	102.4
Spectrin alpha chain, brain	Q13813	2	6.0	9.5	70.4	5.35	284.4
Isoform 2 of Spectrin alpha chain, brain	Q13813-2	2	6.0	8.0	69.6	5.35	284.9
Synapsin-1	P17600	2	5.0	2.3	16.2	9.83	74.1
Tubulin alpha-1A chain	Q71U36	2	58.5	14.0	226.9	5.06	50.1
Tubulin alpha-1B chain	P68363	2	45.7	14.0	222.7	5.06	50.1
Tubulin alpha-4A chain	P68366	2	41.4	11.0	177.4	5.06	49.9
Tubulin beta chain	P07437	2	60.4	16.3	236.5	4.89	49.6
Tubulin beta-2A chain	Q13885	2	62.8	17.5	249.7	4.89	49.9
Tubulin beta-2C chain	P68371	2	60.8	16.3	269.5	4.89	49.8
Tubulin beta-3 chain	Q13509	2	44.2	13.3	138.9	4.93	50.4
Tubulin beta-4 chain	P04350	2	62.8	16.8	268.6	4.88	49.6
Beta-actin variant (fragment)	Q53G99	1	34.1	8.0	147.2	5.59	41.7
Calcium/calmodulin-dependent protein kinase type II subunit beta	Q13554	1	7.2	3.0	17.9	7.27	72.6
Dynactin subunit 1	Q14203	1	3.3	3.0	15.9	5.81	141.6
Dynamin-3	Q9UQ16	1	5.3	4.0	14.8	8.35	97.7
Isoform 2 of Dynamin-1	Q05193-2	1	5.7	3.0	31.4	6.87	97.2
Elongation factor 1-alpha 1	P68104	1	10.1	3.5	32.4	9.01	50.1
Glyceraldehyde-3-phosphate dehydrogenase	P04406	1	8.4	2.0	8.4	8.46	36
Microtubule-associated protein 1A	P78559	1	1.5	3.0	21.1	4.92	305.3
Profilin-1	P07737	1	21.4	2.0	11.1	8.27	15.0
Rab GDP dissociation inhibitor alpha	P31150	1	28.4	7.5	44.8	5.14	50.6

Table 2 (continued)

Protein identified	Accession no.	No. of cases**	Coverage (%)	No. of peptides	Score	pI	MW (kDa)
Spectrin beta chain, brain 1	Q01082	1	5.3	13.5	92.3	5.57	274.4
C: Putative synaptic vesicle proteins							
6-Phosphofructokinase type C	Q01813	2	8.6	5.5	27.1	7.55	85.5
Fructose-bisphosphate aldolase C	P09972	2	13.0	3.3	14.1	6.87	39.4
Gamma-enolase	P09104	2	16.1	4.3	23.4	5.03	47.2
L-lactate dehydrogenase B chain	P07195	2	13.9	3.8	15.1	6.05	36.6
Reticulon-4	Q9NQC3	2	2.7	2.3	13.5	4.5	129.9
6-Phosphofructokinase, liver type	P17858	1	4.5	3.0	15.5	7.50	85.0
Alpha-enolase	P06733	1	17.7	5.0	27.0	7.39	47.1
Phosphoglycerate mutase 1	P18669	1	20.5	3.5	16.4	7.18	28.8
Thy-1 membrane glycoprotein	P04216	1	18.0	2.0	6.8	8.73	17.9

Coverage = average % of the full-length amino acid sequence covered by identified peptides; No. of peptides = average number of unique peptides sequenced; Score = average Xcorr significance score; pI = calculated isoelectric point; MW = calculated molecular weight

*Presence in LBs validated with immunofluorescence (see Fig. 2)

**Number of DLB cases (from which LBs were immunocaptured) in which the protein was identified (out of 2)

Discussion

In this current study, we endeavoured to isolate and enrich LBs and GCIs from human postmortem brains and analyse their protein content through mass spectrometry and immunohistochemistry. Our approach enabled us to identify an array of different proteins within these ASPIs, including an enrichment of vesicle and vesicle-related proteins. This approach to purify these disease-related protein complexes builds on previous work by others in the field. An early study by Pollanen et al. (1993) enriched LBs from DLB tissue using basic sucrose density gradient centrifugation. Iwatsubo et al. (1996) extended this by using a sucrose density gradient followed by fluorescence-activated cell sorting (FACS) using antibodies against ubiquitin and neurofilament. Sian et al. (1998) instead utilised immunomagnetic capture with a primary antibody against either neurofilament or ubiquitin, and a secondary antibody bound to magnetic Dynabeads. Gai et al. (1999) combined and improved features of the previous methods to enrich GCIs from MSA tissue by using a Percoll density gradient followed by immunomagnetic capture with an antibody against α-synuclein, now known to be the main component of GCIs and LBs. This method was subsequently adapted to the purification of LBs from DLB tissue with minor modifications by Jensen et al. (2000). The method of Gai et al. (1999) was improved by McCormack et al. (2016) with modifications including a short protease step to improve the purity and yield of both GCI and LB preparations. The optimised method increased the concentration of the inclusion protein α-synuclein while decreasing the level of contaminating tubulin, with the yield of inclusions from brain homogenate increased over 20-fold (McCormack et al. 2016). This approach was subsequently utilised is this current study.

One hypothesis behind the role of inclusions in the cell is that inclusion formation is a protective mechanism that sequesters potentially toxic excess or misfolded α-synuclein that cannot be degraded by the cell (Wakabayashi et al. 2007). Given that ASPIs are large and centrally located in the cell, it is likely that ASPI proteins including α-synuclein will need to be transported to the ASPI. Identifying the proteome of LBs and GCIs may elucidate which proteins are involved in the packaging and transport of α-synuclein into inclusions and potentially the pathway by which this occurs. While α-synuclein is present in neurons and thus may be incorporated into LBs through numerous mechanisms, α-synuclein is not expressed in oligodendrocytes (Miller et al. 2005) which support the selective targeting of this protein to GCIs.

Overabundant or misfolded proteins would normally be degraded by either the ubiquitin–proteasome system (UPS) or the autophagy–lysosomal pathway (ALP). Defects in any of the enzymes involved in either the UPS or ALP may lead to a reduction in capacity for clearing damaged proteins. If this is combined with an excess of aggregated α-synuclein, the aggregated α-synuclein may continue to form at a rate faster than which it can be cleared from the cytosol. UPS proteins identified in this study in both GCIs (≥ 4 out of 5 cases) and LBs (2 out of 2 cases) include the 26S protease regulatory subunit 7, UCH-L1 (also identified by Leverenz et al. 2007), ubiquitin-like modifier-activating enzyme 1 (also identified by Leverenz et al. 2007), ubiquitin carboxy-terminal hydrolase 5 and polyubiquitin C. The lysosomal marker lysosome membrane protein 2 (LAMP2) was identified in GCIs (≥ 4 out of 5 cases) but not in LBs.

There is also a proposed link between mitochondrial dysfunction and neurodegenerative disorders, with both chemical and genetic evidence for mitochondrial involvement in

Table 3 MS/MS results of proteins from immunocaptured glial cytoplasmic inclusions (GCIs) that are synaptic vesicle-related proteins

Protein identified	Accession no.	No. of cases**	Coverage (%)	No. of peptides	Score	pI	MW (kDa)
A: Established synaptic vesicle proteins							
Synaptosomal-associated protein 25*	P60880	5	25.5	3.9	20.2	4.77	23.3
V-type proton ATPase catalytic subunit A	P38606	4	12.3	4.8	35.6	5.52	68.3
V-type proton ATPase subunit d 1	P61421	4	20.1	3.7	24.5	5.00	40.3
V-type proton ATPase subunit B, brain isoform	P21281	4	11.6	3.6	21.0	5.81	56.5
Ras-related protein Rab-3A	P20336	3	23.6	3.8	18.8	5.03	25.0
Synaptotagmin-1*	P21579	2	13.8	4.5	27.7	8.12	47.5
Synaptophysin*	P08247	2	8.0	2.0	16.2	4.81	33.8
Vesicle-associated membrane protein 2*	P63027	2	28.5	2.0	14.6	8.13	12.7
Synaptic vesicle glycoprotein 2A	Q7L0J3	2	3.3	2.3	10.8	5.57	82.6
Syntaxin-1B	P61266	2	11.7	2.3	16.3	5.38	33.2
Syntaxin-1A	Q16623	1	7.6	2.0	7.2	5.24	33.0
Synaptogyrin-1	O43759	1	10.3	2.0	5.9	4.68	25.4
V-type proton ATPase subunit E 1	P36543	1	11.1	2.0	10.5	8.00	26.1
V-type proton ATPase subunit H	Q9UI12	1	6.6	2.0	6.7	6.48	55.8
V-type proton ATPase subunit F	Q16864	1	26.1	2.0	6.4	5.52	13.4
B: Transiently-associated with the synaptic vesicle membrane							
Tubulin beta-4 chain	P04350	5	56.0	16.3	290.1	4.88	49.6
Tubulin beta-2C chain	P68371	5	54.0	16.0	250.8	4.89	49.8
Tubulin beta-2A chain	Q13885	5	53.3	15.7	234.0	4.89	49.9
Tubulin alpha-1A chain	Q71U36	5	58.7	14.1	228.7	5.06	50.1
Tubulin beta chain	P07437	5	50.8	15.0	224.3	4.89	49.6
Tubulin alpha-1B chain	P68363	5	58.4	14.0	217.6	5.06	50.1
Tubulin beta-3 chain	Q13509	5	37.9	11.9	119.0	4.93	50.4
Heat shock protein HSP 90-beta	P08238	5	21.7	12.5	100.7	5.03	83.2
Cytoplasmic dynein 1 heavy chain 1	Q14204	5	3.9	12.8	95.9	6.40	532.0
Heat shock protein HSP 90-alpha	P07900	5	22.2	11.8	85.9	5.02	84.6
Neurofilament medium polypeptide	P07197	5	13.2	8.4	78.0	4.91	102.4
Neurofilament light polypeptide	P07196	5	19.5	7.5	71.8	4.65	61.5
Clathrin heavy chain 1	Q00610	5	7.7	8.8	60.2	5.69	191.5
Alpha-internexin	Q16352	5	17.0	6.5	55.6	5.40	55.4
Microtubule-associated protein 1B	P46821	5	5.1	8.6	43.0	4.81	270.5
Elongation factor 1-alpha 1	P68104	5	10.7	3.7	33.6	9.01	50.1
Beta-soluble NSF attachment protein	Q9H115	5	28.0	5.6	29.1	5.47	33.5
Glyceraldehyde-3-phosphate dehydrogenase	P04406	5	12.0	2.6	11.7	8.46	36.0
Tubulin alpha-4A chain	P68366	4	40.0	10.3	195.3	5.06	49.9
Actin, cytoplasmic 1	P60709	4	34.2	7.6	113.9	5.48	41.7
Spectrin beta chain, brain 1	Q01082	4	5.4	8.8	60.2	5.57	274.4
Isoform 2 of Dynamin-1	Q05193-2	4	12.3	7.0	49.4	6.87	97.2
Calcium/calmodulin-dependent protein kinase II alpha	Q8IWE0	4	16.0	4.5	30.9	7.20	54.1
Synapsin-1	P17600	4	7.2	2.8	22.7	9.83	74.1
Calcium/calmodulin-dependent protein kinase type II subunit delta	Q13557	4	12.9	3.7	21.7	7.25	56.0
Isoform 2 of Spectrin alpha chain, brain	Q13813–2	3	6.0	9.2	62.9	5.35	284.9
Neurofilament heavy polypeptide	P12036	3	7.7	6.3	50.2	6.18	112.4
Elongation factor 1-alpha	A8K9C4	3	13.9	4.3	44.8	9.01	50.2
Rab GDP dissociation inhibitor alpha	P31150	3	22.4	6.2	31.5	5.14	50.6
Calcium/calmodulin-dependent protein kinase type II subunit beta	Q13554	3	7.6	3.3	24.2	7.27	72.6
AP-2 complex subunit beta	P63010	3	4.3	2.3	15.8	5.38	104.5
AP-2 complex subunit alpha-1	O95782	3	3.2	2.0	9.6	7.03	107.5
Tubulin polymerisation-promoting protein	O94811	3	17.8	2.0	9.2	9.44	23.7
Beta-actin variant (fragment)	Q53G99	2	31.5	6.7	87.5	5.59	41.7
Dynamin-3	Q9UQ16	2	4.3	3.0	21.8	8.35	97.7
Isoform delta 6 of calcium/calmodulin-dependent protein kinase type II subunit delta	Q13557-8	2	10.6	2.5	21.1	7.25	54.1
Microtubule-associated protein 1A	P78559	2	1.7	3.5	20.1	4.92	305.3
Isoform 8 of calcium/calmodulin-dependent protein kinase type II subunit beta	Q13554-8	2	11.7	3.5	17.5	7.28	57.9
Elongation factor 1-delta	P29692	2	9.8	2.3	10.8	5.01	31.1
Tubulin beta-6 chain	Q9BUF5	1	23.7	8.0	179.6	4.88	49.8
Isoform 2 of heat shock protein HSP 90-alpha	P07900-2	1	26.0	17.0	125.4	5.16	98.1
Elongation factor 1-alpha (fragment)	Q53G85	1	9.7	3.0	27.4	9.01	50.1
Dynamin-2	P50570	1	5.3	4.0	25.0	7.44	98.0
Dynamin-1	Q05193	1	3.4	2.0	19.6	7.17	97.3
Spectrin alpha chain, brain	Q13813	1	1.4	2.0	18.6	5.35	284.4
Dynactin subunit 1	Q14203	1	2.7	2.0	14.8	5.81	141.6
Synapsin-2	Q92777	1	9.6	3.0	14.1	8.41	62.8

Table 3 (continued)

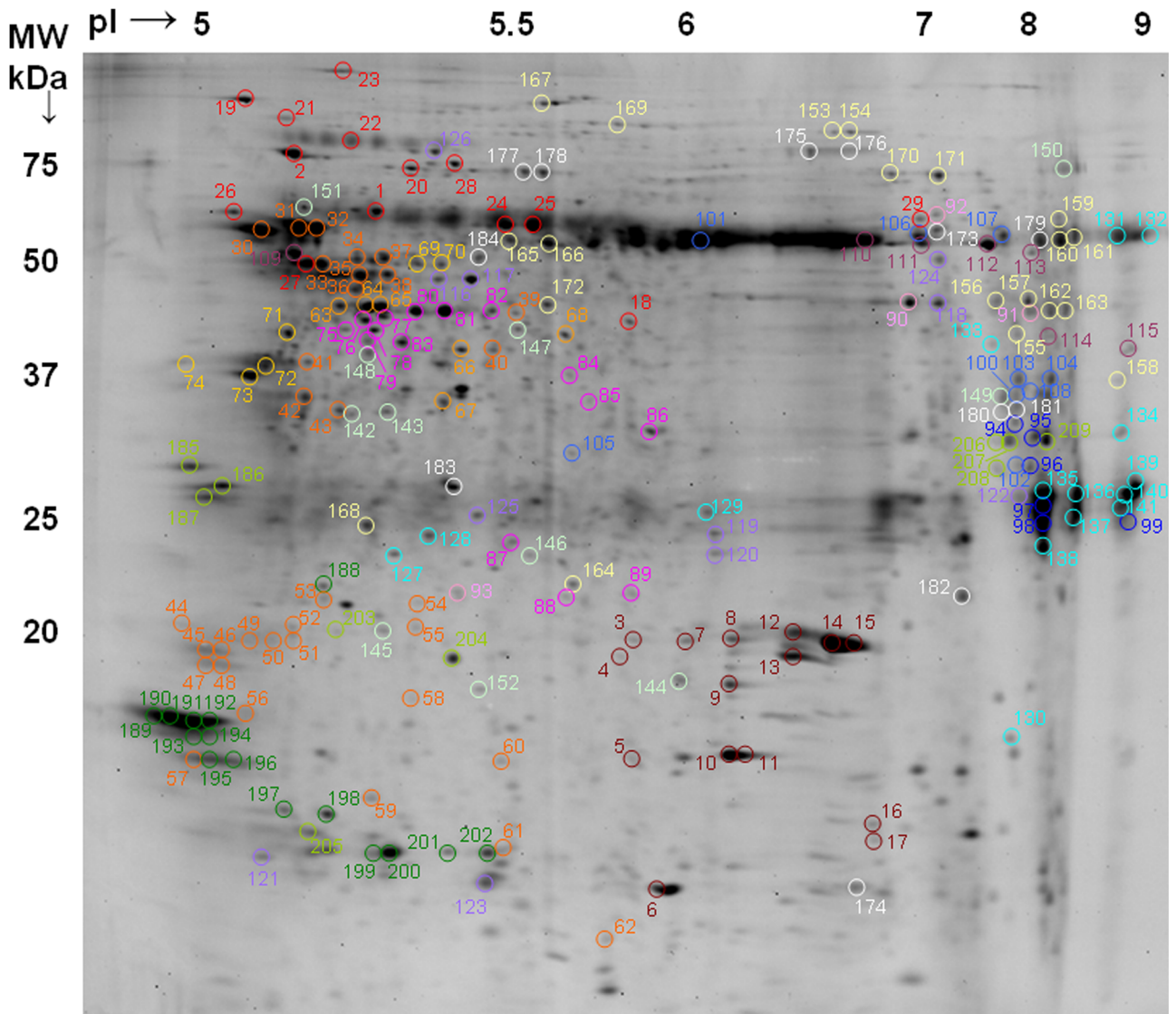| Protein identified	Accession no.	No. of cases**	Coverage (%)	No. of peptides	Score	pI	MW (kDa)
Profilin-1	P07737	1	21.4	2.0	13.6	8.27	15.0
Dynamin 1 isoform 2 variant (fragment)	Q59GI5	1	4.0	2.0	13.0	7.68	68.8
Dynamin-1-like protein	O00429	1	3.5	2.0	12.3	6.81	81.8
Elongation factor 1-gamma	P26641	1	7.1	2.0	10.6	6.67	50.1
Alpha-soluble NSF attachment protein	P54920	1	14.2	3.0	10.1	5.36	33.2
Highly similar to Dynactin-1	B4DM45	1	2.4	2.0	9.2	5.40	136.7
AP-2 complex subunit alpha-2	O94973	1	3.3	2.0	9.0	6.96	103.9
Dynein light chain 1, cytoplasmic	P63167	1	37.1	2.0	8.2	7.40	10.4
Mitochondrial dynamin-like 120 kDa protein	E5KLK2	1	3.4	2.0	7.4	7.99	107.5
C: Putative synaptic vesicle proteins							
Phosphoglycerate mutase 1	P18669	4	20.9	3.6	23.2	7.18	28.8
Reticulon-4	Q9NQC3	4	5.1	3.1	20.7	4.50	129.9
Gamma-enolase	P09104	4	17.4	4.4	20.0	5.03	47.2
L-lactate dehydrogenase B chain	P07195	4	8.4	2.3	12.4	6.05	36.6
6-Phosphofructokinase type C	Q01813	3	10.5	5.3	26.8	7.55	85.5
Rap1 GTPase-GDP dissociation stimulator 1	P52306	3	9.8	4.0	24.5	5.31	66.3
Alpha-enolase	P06733	3	13.4	3.5	20.6	7.39	47.1
6-Phosphofructokinase, muscle type	P08237	3	5.8	3.6	18.0	7.99	85.1
Ras-related protein Rab-2A	P61019	3	14.6	2.3	12.1	6.54	23.5
6-Phosphofructokinase, liver type	P17858	2	8.2	4.7	24.8	7.50	85.0
Thy-1 membrane glycoprotein	P04216	2	18.0	2.0	13.5	8.73	17.9
Isoform 3 of Reticulon-3	O95197-3	2	11.0	2.0	10.7	8.51	25.6
Visinin-like protein 1	P62760	1	24.6	4.0	16.2	5.15	22.1
Ras-related protein Rab-1A	P62820	1	22.4	3.0	14.0	6.21	22.7
Pyruvate kinase isozymes M1/M2	P14618	1	5.7	2.0	11.8	7.84	57.9
Ras-related protein Rab-11A	P62491	1	11.1	2.0	9.8	6.57	24.4
Septin-7	Q16181	1	6.5	2.0	9.0	8.63	50.6
Ras-related protein Rab-5C	P51148	1	10.7	2.0	8.4	8.41	23.5
Fructose-bisphosphate aldolase C	P09972	1	8.5	2.0	7.5	6.87	39.4

*Presence in GCIs validated with immunofluorescence (see Fig. 2)

**Number of MSA cases (from which GCIs were immunocaptured) in which the protein was identified (out of 5)

the pathogenesis of PD (Bender et al. 2006; Chen and Chan 2009; Kraytsberg et al. 2006; Onyango 2008; Smeyne and Jackson-Lewis 2005). Eleven electron transport chain proteins were identified in this study in GCIs (≥4 out of 5 cases), including components of complex I/NADH dehydrogenase complex (3 proteins), complex III/cytochrome b complex (3 proteins), complex IV/cytochrome oxidase complex (1 protein) and complex V/ATP synthase complex (4 proteins). Six of these proteins were also identified in LBs. Shahmoradian et al. (2017) used advanced electron microscopy techniques to visualise LBs from postmortem brain tissue, which revealed a medley of membranous structures, such as vesicles, lysosomes and dysmorphic mitochondria. This supports the hypothesis that impaired organelle trafficking in the mitochondrial and/or lysosomal pathways contributes to the pathogenesis of Parkinson's disease. Furthermore, there exist clear links between proper mitochondrial function, neurotransmission and neurodegeneration Peiris et al. 2014), with reduced transmission observed in models of Parkinson's disease prior to the development of overt symptoms or degeneration (Keating 2008).

Indeed, after vesicle-associated proteins, energy transduction proteins and chaperones were also highly represented. In this study, we have focused on vesicle associated proteins because they are the most abundant group of proteins and because of their potential to explain how alpha synuclein is transported both to LBs and to GCIs. Consequently, an attractive hypothesis for the formation of inclusions is that aggregated α-synuclein is selectively targeted to inclusions via vesicle-mediated transport. It is proposed that there is a pathway involving the release of toxic α-synuclein species from neurons, a reuptake of α-synuclein from the extracellular space by neighbouring neurons (in PD and DLB) or oligodendrocytes (in MSA), and the targeting and intracellular trafficking of α-synuclein through retrograde vesicular transport to

Fig. 1 Representative 2-DE gel image of solubilised proteins from ▶ immunocaptured GCIs. Two hundred fifty micrograms of inclusions purified using the optimised GCI purification method were subjected to 2-DE using a 24 cm pH 3-11NL strip and 12.5% linear SDS-PAGE. The gel was stained with SyproRuby and imaged on a Typhoon 9400 variable mode imager. Selected spots were identified by Thermo LTQ Orbitrap XL mass spectrometry
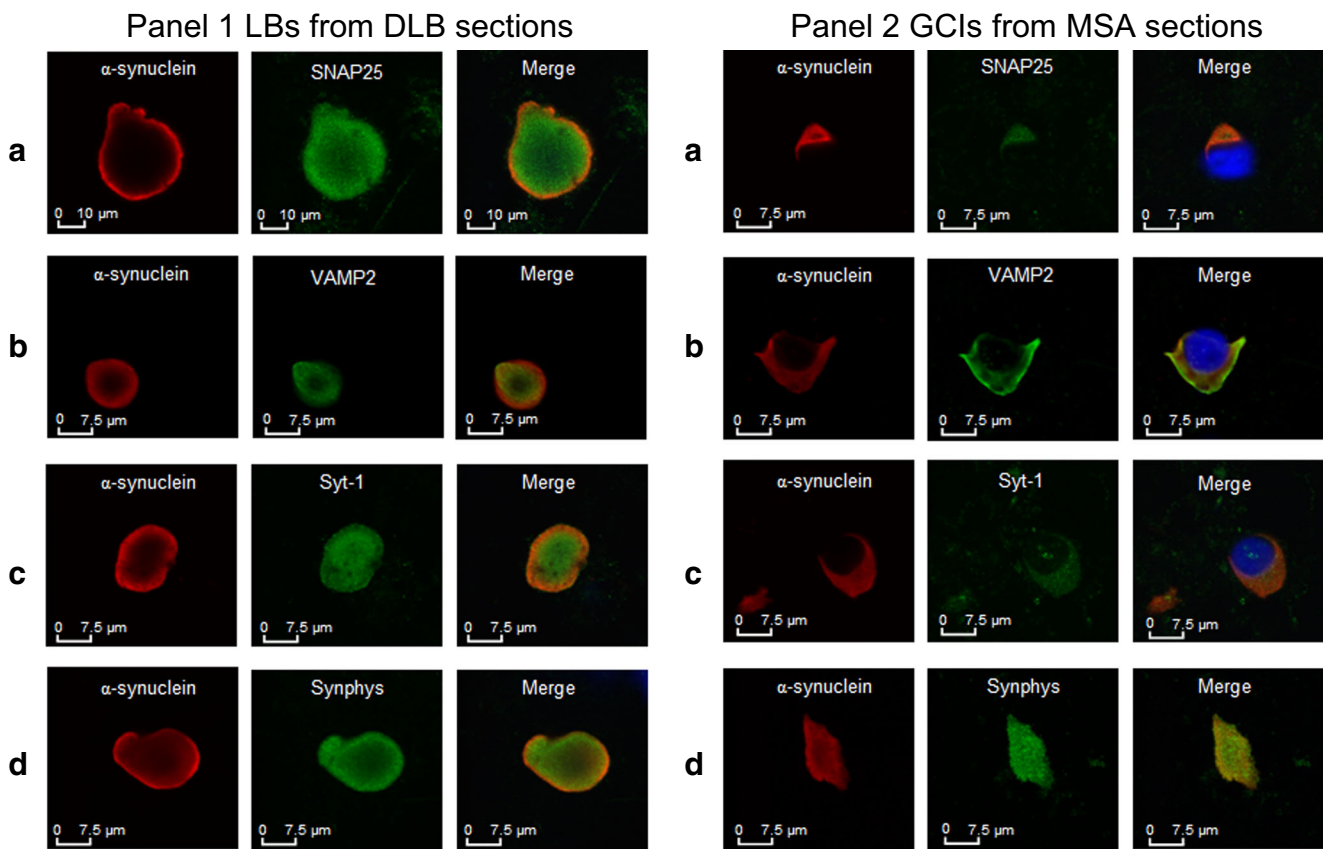
Fig. 2 Immunofluorescence validation of the presence of synaptic vesicle-related proteins in Lewy bodies (LBs) and glial cytoplasmic inclusions (GCIs). Fixed sections of DLB tissue (panel 1) and MSA tissue (panel 2) were dual stained against α-synuclein and (A) SNAP25, (B) VAMP2, (C) synaptotagmin 1 and (D) synaptophysin. A Cy-3-conjugated secondary antibody was used for α-synuclein, appearing red, and an Alexa-488-conjugated secondary antibody was used for the synaptic vesicle proteins, appearing green. In the MSA sections, nuclei were stained with DAPI and appear blue

the inclusion within the cell body (Fig. 3). When the 174 consistently identified LB proteins (2/2 cases) were compared to the 164 consistently identified GCI proteins ($\geq 4/5$ cases), 112 of the proteins were common to both LBs and GCIs. Twenty-five of these 112 proteins (22%) had previously been established as components of LBs or GCIs. Twenty-eight of these 112 proteins (25%) were synaptic vesicle-related, of which 12 proteins have not previously been established as LB or GCI proteins, including the synaptic vesicle-related protein SNAP-25. A vesicle-based trafficking mechanism could explain the presence of the wide range of vesicle-related proteins identified from inclusions in this study and a common formation mechanism for LBs and GCIs. An alternative hypothesis, which cannot be discounted, is that vesicle-related proteins are present in inclusions as a result of their interaction with α-synuclein.

Of the 112 proteins consistently identified between GCIs and brainstem LBs in this study, 45 proteins (40%) were also identified in cortical bodies in a study by Leverenz et al. (2007). The 91 proteins (out of 156) identified by Leverenz et al. (2007) that were not consistently identified in either GCIs or LBs in this study may arise for two reasons. Firstly,

the sample analysed by Leverenz et al. (2007) was a single pooled sample from five DLB cases, so an identified protein may have arisen from only one or two of the contributing cases instead of being common to all cases. The data was not compared to the identifications made from single cases in this study. Secondly, these proteins may be present as contaminants from the surrounding tissue because of the laser capture process used for inclusion purification by Leverenz et al. (2007). As LBs were captured from 10 μm sections of tissue, and LBs are spherical in structure, the tissue immediately surrounding the LBs would also be captured and the proteins from this tissue identified in the sample alongside the genuine LB proteins.

A wide range of proteins across a variety of functional groups were identified with 2-DE separation and mass spectrometry of selected spots. While no established synaptic vesicle proteins were identified from the analysed spots, several proteins with a protein trafficking function were identified. Low molecular weight synaptic vesicle proteins are easily missed with 2-DE/MS, as there are fewer peptides present in low molecular weight proteins to identify and greater losses during washing and handling steps due to their small mass.
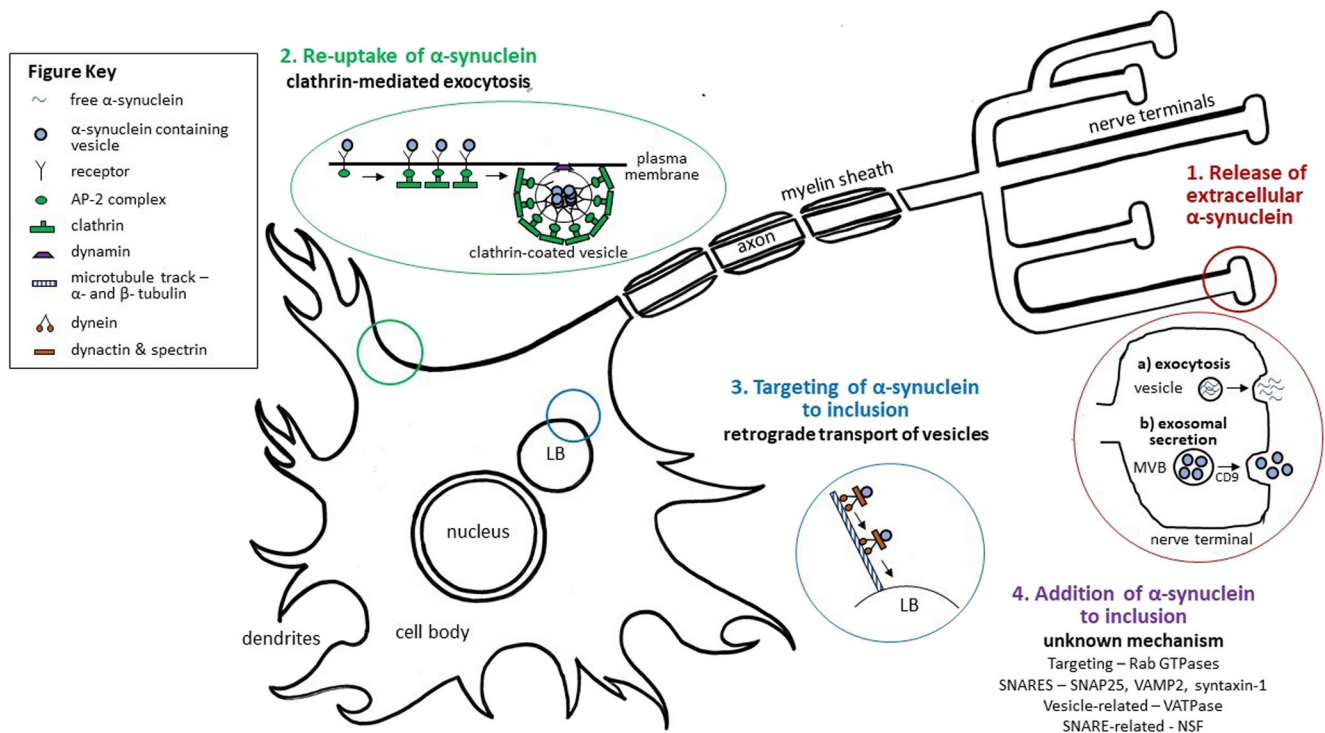
Fig. 3 Proposed mechanism of inclusion formation via vesicle-mediated transport of α-synuclein. Step 1: the release of external α-synuclein from the presynaptic nerve terminal is proposed to occur via either exocytosis of free α-synuclein, or via the release of α-synuclein-containing exosomes from a multi-vesicular body (MVB) (supported by the identification of exosomal marker CD9 in LBs). Step 2: the re-uptake of extracellular α-synuclein into the cell body is proposed to occur by clathrin-mediated endocytosis (supported by the identification of clathrin, AP-2 complex subunits, and dynamin). Step 3: specific targeting of α-synuclein to the inclusion is proposed to occur by retrograde vesicular transport along microtubule tracks (supported by the identification of dynein, α- and β-tubulin, dynactin and spectrin). Step 4: the addition of α-synuclein and associated proteins to the inclusion is proposed to involve SNARE proteins, mechanism unknown (supported by the identification of Rab GTPases, SNAP25, VAMP2, syntaxin-1, VATPase and NSF). Note: while the re-uptake of α-synuclein (steps 2–4) is shown in this diagram on the same neuron from which it is released (step 1) for the sake of clarity, the reuptake is proposed to take place by neighbouring neurons (in DLB and PD) or oligodendrocytes (in MSA)

Also, many vesicle proteins have transmembrane regions; thus, their hydrophobic nature may cause them to focus poorly via 2D-E and therefore their identification missed on a 2D gel.

Immunofluorescence was used to provide an independent verification of the presence of some of the key identifications made by mass spectrometry. SNAP-25, VAMP2, synaptotagmin I and synaptophysin were selected for validation based on their classification as established synaptic vesicle-related proteins and commercial antibody availability. Synaptophysin was found in LBs via immunofluorescence despite not being detected in the two DLB samples analysed by mass spectrometry. The lack of detection by MS can be due to many reasons including lack of tryptic cleavage sites, glycoslylation, poor chromatography/ ionisation of peptides, incomplete fragmentation of peptides and ion suppression from other coeluting ions. It may have been below the limit of detection for a complex mixture in the two samples analysed. As it was identified in only two out of the five MSA samples analysed, it may have been detected in LBs if a larger number of cases were analysed.

The proteins that were consistently identified in GCIs and LBs in this study have been used as the basis for developing two alternative hypotheses for how proteins are targeted to inclusions. Defective α-synuclein and associated proteins may be released extracellularly from the presynaptic terminal, for reuptake by the target cell in clathrin-coated vesicles (neurons in PD or DLB, oligodendrocytes in MSA), where they are selectively targeted to an inclusion body via retrograde vesicular transport. The identification of a large number of synaptic vesicle-related proteins in the purified GCI and LB samples in this study, including those associated with exosomes (CD9), clathrin-mediated endocytosis (clathrin, AP-2 complex, dynamin), retrograde transport (dynein, dynactin, spectrin) and synaptic vesicle fusion (SNAP25, VAMP2, syntaxin-1), supports this hypothesis (see Fig. 3).

Alternatively, misfolded or excess α-synuclein may lead to an inhibition of ER-Golgi trafficking and subsequent ER stress at the point of translation, where α-synuclein and associated proteins that subsequently fail to be degraded are targeted to a LB via anterograde transport in COPII-coated vesicles. While

the ER chaperone proteins GRP78, PDI, calnexin and calreticulin were identified in this study, proteins relating to the UPR signalling cascade and the formation of COPII-vesicles (with the exception of the supporting family of p24 proteins) were not identified in purified inclusions. Furthermore, it is unclear how the latter mechanism would relate to GCI formation in MSA, as the α-synuclein would still need to be targeted to the oligodendrocyte from a neuronal cell.

In summary, this study has provided a comprehensive characterisation of the ASPI proteome, now possible due to the recent development of an improved ASPI purification method. The finding that 21% of proteins consistently identified in both LB samples and glial cytoplasmic inclusion samples are synaptic vesicle-related supports the hypothesis that misfolded α-synuclein is trafficked in vesicles to a central inclusion body as the common formation mechanism for both LBs and GCIs.

Publisher's Note Springer Nature remains neutral with regard to jurisdictional claims in published maps and institutional affiliations.

References

Alves G, Forsaa EB, Pedersen KF, Dreetz Gjerstad M, Larsen JP (2008) Epidemiology of Parkinson's disease. J Neurol 255(Suppl 5):18–32

Bender A, Krishnan KJ, Morris CM, Taylor GA, Reeve AK, Perry RH, Jaros E, Hersheson JS, Betts J, Klopstock T, Taylor RW, Turnbull DM (2006) High levels of mitochondrial DNA deletions in substantia nigra neurons in aging and Parkinson disease. Nat Genet 38:515–517

Borghi R, Marchese R, Negro A, Marinelli L, Forloni G, Zaccheo D, Abbruzzese G, Tabaton M (2000) Full length alpha-synuclein is present in cerebrospinal fluid from Parkinson's disease and normal subjects. Neurosci Lett 287:65–67

Burre J, Volknandt W (2007) The synaptic vesicle proteome. J Neurochem 101:1448–1462

Chen H, Chan DC (2009) Mitochondrial dynamics—fusion, fission, movement, and mitophagy—in neurodegenerative diseases. Hum Mol Genet 18:R169–R176

Cordato DJ, Chan DK (2004) Genetics and Parkinson's disease. J Clin Neurosci 11:119–123

Culvenor JG, Rietze RL, Bartlett PF, Masters CL, Li QX (2002) Oligodendrocytes from neural stem cells express alpha-synuclein: increased numbers from presenilin 1 deficient mice. Neuroreport 13: 1305–1308

Fahn S (2003) Description of Parkinson's disease as a clinical syndrome. Ann N Y Acad Sci 991:1–14

Gai WP, Power JH, Blumbergs PC, Culvenor JG, Jensen PH (1999) Alpha-synuclein immunoisolation of glial inclusions from multiple system atrophy brain tissue reveals multiprotein components. J Neurochem 73:2093–2100

Inoue M, Yagishita S, Ryo M, Hasegawa K, Amano N, Matsushita M (1997) The distribution and dynamic density of oligodendroglial cytoplasmic inclusions (GCIs) in multiple system atrophy: a correlation between the density of GCIs and the degree of involvement of striatonigral and olivopontocerebellar systems. Acta Neuropathol 93:585–591

Iwatsubo T, Yamaguchi H, Fujimuro M, Yokosawa H, Ihara Y, Trojanowski JQ, Lee VM (1996) Purification and characterization of Lewy bodies from the brains of patients with diffuse Lewy body disease. Am J Pathol 148:1517–1529

Jensen PH, Islam K, Kenney J, Nielsen MS, Power J, Gai WP (2000) Microtubule-associated protein 1B is a component of cortical Lewy bodies and binds alpha-synuclein filaments. J Biol Chem 275: 21500–21507

Jin LT, Hwang SY, Yoo GS, Choi JK (2006) A mass spectrometry compatible silver staining method for protein incorporating a new silver sensitizer in sodium dodecyl sulfate-polyacrylamide electrophoresis gels. Proteomics 6:2334–2337

Keating DJ (2008) Mitochondrial dysfunction, oxidative stress, regulation of exocytosis and their relevance to neurodegenerative diseases. J Neurochem 104:298–305

Klein C, Schlossmacher MG (2007) Parkinson disease, 10 years after its genetic revolution: multiple clues to a complex disorder. Neurology 69:2093–2104

Kraytsberg Y, Kudryavtseva E, McKee AC, Geula C, Kowall NW, Khrapko K (2006) Mitochondrial DNA deletions are abundant and cause functional impairment in aged human substantia nigra neurons. Nat Genet 38:518–520

Leverenz JB, Umar I, Wang Q, Montine TJ, McMillan PJ, Tsuang DW, Jin J, Pan C, Shin J, Zhu D, Zhang J (2007) Proteomic identification of novel proteins in cortical lewy bodies. Brain Pathol 17:139–145

Licker V, Kovari E, Hochstrasser DF, Burkhard PR (2009) Proteomics in human Parkinson's disease research. J Proteome 73:10–29

Lindersson E, Lundvig D, Petersen C, Madsen P, Nyengaard JR, Højrup P, Moos T, Otzen D, Gai WP, Blumbergs PC, Jensen PH (2005) p25alpha Stimulates alpha-synuclein aggregation and is co-localized with aggregated alpha-synuclein in alpha-synucleinopathies. J Biol Chem 280:5703–5715

Link AJ, LaBaer J (2009) Proteomics: a Cold Spring Harbor laboratory course manual. Cold Spring Harbor laboratory press, Cold Spring Harbor

McCormack A, Chegeni N, Chegini F, Colella A, Power J, Keating D, Chataway T (2016) Purification of alpha-synuclein containing inclusions from human post mortem brain tissue. J Neurosci Methods 266:141–150

McKeith I, Mintzer J, Aarsland D, Burn D, Chiu H, Cohen-Mansfield J, Dickson D, Dubois B, Duda JE, Feldman H, Gauthier S, Halliday G, Lawlor B, Lippa C, Lopez OL, Carlos Machado J, O'Brien J, Playfer J, Reid W, International Psychogeriatric Association Expert Meeting on DLB (2004) Dementia with Lewy bodies. Lancet Neurol 3:19–28

Miller DW, Johnson JM, Solano SM, Hollingsworth ZR, Standaert DG, Young AB (2005) Absence of alpha-synuclein mRNA expression in normal and multiple system atrophy oligodendroglia. J Neural Transm 112:1613–1624

Onyango IG (2008) Mitochondrial dysfunction and oxidative stress in Parkinson's disease. Neurochem Res 33:589–597

Ozawa T (2006) Pathology and genetics of multiple system atrophy: an approach to determining genetic susceptibility spectrum. Acta Neuropathol 112:531–538

Peiris H, Dubach D, Jessup CF, Unterweger P, Raghupathi R, Muyderman H, Zanin MP, Mackenzie K, Pritchard MA, Keating DJ (2014) RCAN1 regulates mitochondrial function and increases susceptibility to oxidative stress in mammalian cells. Oxidative Med Cell Longev 2014:520316

Pollanen MS, Bergeron C, Weyer L (1993) Deposition of detergent-resistant neurofilaments into Lewy body fibrils. Brain Res 603:121–124

Richter-Landsberg C, Gorath M, Trojanowski JQ, Lee VM (2000) Alpha-synuclein is developmentally expressed in cultured rat brain oligodendrocytes. J Neurosci Res 62:9–14

Shahmoradian SH, Genoud C, Graff-Meyer A, Hench J, Moors T, Schweighauser G, Wang J, Goldie KN, Suetterlin R, Castano-Diez D, Perez-Navarro P, Huisman E, Ipsen S, Ingrassia A, De Gier Y, Rozemuller AJ, Da Paepe A, Erny J, Staempfli A, Hoernschemeyer J, Grosserueschkamp F, Niedieker D, El-Mashtoly S, Quadri M, Van WF, Bonifati V, Gerwert K, Bohrmann B, Frank A, Britschgi M, Stahlberg H, Berg VD, Lauer ME (2017) Lewy pathology in Parkinson's disease consists of a crowded organellar membranous medley. Cold Spring Harbor Laboratory Press, Cold Spring Harbor

Sian J, Hensiek R, Senitz D, Muench G, Jellinger K, Riederer P, Gerlach M (1998) A novel technique for the isolation of Lewy bodies in brain. Acta Neuropathol 96:111–115

Smeyne RJ, Jackson-Lewis V (2005) The MPTP model of Parkinson's disease. Brain Res Mol Brain Res 134:57–66

Tan EK (2007) The role of common genetic risk variants in Parkinson disease. Clin Genet 72:387–393

Uversky VN, Eliezer D (2009) Biophysics of Parkinson's disease: structure and aggregation of alpha-synuclein. Curr Protein Pept Sci 10:483–499

Vanacore N (2005) Epidemiological evidence on multiple system atrophy. J Neural Transm 112:1605–1612

Vanacore N, Bonifati V, Fabbrini G, Colosimo C, de Michele G, Marconi R, Nicholl D, Locuratolo N, Talarico G, Romano S, Stocchi F, Bonuccelli U, de Mari M, Vieregge P, Meco G, European Study Group on Atypical Parkinsonism (ESGAP) (2001) Epidemiology of multiple system atrophy. ESGAP Consortium. European Study Group on Atypical Parkinsonisms. Neurol Sci 22:97–99

Wakabayashi K, Takahashi H (2006) Cellular pathology in multiple system atrophy. Neuropathology 26:338–345

Wakabayashi K, Tanji K, Mori F, Takahashi H (2007) The Lewy body in Parkinson's disease: molecules implicated in the formation and degradation of alpha-synuclein aggregates. Neuropathology 27:494–506

Wenning GK, Tison F, Ben Shlomo Y, Daniel SE, Quinn NP (1997) Multiple system atrophy: a review of 203 pathologically proven cases. Mov Disord 12:133–147

Wenning GK, Stefanova N, Jellinger KA, Poewe W, Schlossmacher MG (2008) Multiple system atrophy: a primary oligodendrogliopathy. Ann Neurol 64:239–246

Wilson CH, Zeile S, Chataway T, Nieuwenhuijs VB, Padbury RT, Barritt GJ (2011) Increased expression of peroxiredoxin 1 and identification of a novel lipid-metabolizing enzyme in the early phase of liver ischemia reperfusion injury. Proteomics 11:4385–4396

Wood-Kaczmar A, Gandhi S, Wood NW (2006) Understanding the molecular causes of Parkinson's disease. Trends Mol Med 12:521–528

Yoshida M (2007) Multiple system atrophy: alpha-synuclein and neuronal degeneration. Neuropathology 27:484–493